International Journal of Heat and Mass Transfer 55 (2012) 4908–4913

Contents lists available at SciVerse ScienceDirect

International Journal of Heat and Mass Transfer

journal homepage: www.elsevier.com/locate/ijhmt

Technical Note

A vapor chamber using extended condenser concept for ultra-high heat flux and large heater area

Xianbing Ji [a], Jinliang Xu [b,*], Aime Marthial Abanda [c], Qiang Xue [c]

[a] State Key Laboratory of Alternate Electrical Power System with Renewable Energy Sources, North China Electric Power University, Beijing 102206, PR China
[b] The Beijing Key Laboratory of New and Renewable Energy, North China Electric Power University, Beijing 102206, PR China
[c] The Beijing Key Laboratory of Multiphase Flow and Heat Transfer, North China Electric Power University, Beijing 102206, PR China

ARTICLE INFO

Article history:
Received 21 November 2011
Received in revised form 8 April 2012
Accepted 9 April 2012
Available online 12 May 2012

Keywords:
Vapor chamber
Ultra-high heat flux
Extended condenser
Copper foam

ABSTRACT

We proposed an extended vapor chamber (EVC), consisting of an evaporator part and an extended condenser part. A layer of compressed copper foam was sintered on the inner evaporator surface. The extended condenser includes a circular-straight groove network and a fin region. The groove network distributes generated vapor everywhere in the internal volume of EVC. A set of capillary holes are machined within fins. A sliced copper foam bar is inserted in each of capillary hole. The peaks of copper foam bar are tightly contacted with the evaporator copper foam piece. Water is used as the working fluid with a heater area of 0.785 cm^2. A minimum thermal resistance of 0.03 K/W is reached for the bottom heating. The heat flux is up to 450 W/cm^2 without reaching dryout. The transition point of thermal resistances versus heat fluxes is significantly delayed with the heat flux exceeding 300 W/cm^2, beyond which thermal resistances are only slightly increased. EVC not only improves temperature uniformity on the evaporator and fin base surfaces, but also evens the temperature distribution along the fin height direction to increase the fin efficiency. Inclination angles and charge ratios are combined to affect the thermal performance of EVC. An optimal charge ratio of 0.3 was recommended. EVC can be used for ultra-high heat flux and larger heater area conditions.

1. Introduction

The performance, reliability, and lifetime of electronic devices are dependent on the temperature. The light-emitting diodes (LEDs) have distinct advantages of energy saving, long lifetime, quick response time and compact size. However, the high temperature at high heat flux is a major barrier to fully enjoy the advantages of LEDs. The heat flux for LED chips reaches more than 100 W/cm^2 at this stage, inducing high hot spot temperature if conventional cooling technique is used [1].

A vapor chamber, also called a planar heat pipe, can sustain high heat flux and even the temperature distribution on a flat plate surface. A vapor chamber is a two-phase heat transfer device. The inner wick on the bottom wall in contact with the electronic chips serves as the evaporator, where the liquid evaporates and carries heat away from the heating surface. The upper wall functions as the condenser where the vapor condenses and releases the latent heat, which is dissipated out through the adjacent fin heat sink. The condensed liquid is recycled back to the evaporator by capillary force.

Various designs of vapor chambers were proposed in the literature. Agata et al. [2] fabricated a vapor chamber for notebook computers. The heating area is 2 by 2 cm. The thermal resistance of the vapor chamber was about 0.15 K/W. Wu et al. [3] studied vapor chambers using conventional design with the inner surface covered with copper powder wick, for cooling high-density blade servers. The working fluid is water. Take et al. [4] fabricated roll bond aluminum vapor chamber as the heat spreader for notebook computers. The internal groove corners were used as the capillary structure for liquid transport. R-134a or R-123 was used as the working fluid. The thermal resistance of the vapor chamber was not reported. Lee et al. [5] studied a vapor chamber with a boiling-enhanced multi-wick structure. The vapor chamber resistance could be as low as 0.04–0.03 K/W for heat loads of 100–330 W with a 2.5 × 2.5 cm heater and a heat sink footprint of 9.0 × 8.8 cm.

Recently, Hwang et al. [6] designed and tested a multi-artery heat-pipe spreader vapor chamber. Liquid (water) is transported to a locally high heat flux region through a monolayer evaporator wick and a set of lateral converging arteries, fabricated from sintered, spherical copper particles. A continuous liquid supply through the lateral arteries does not allow for total dryout in the test limit of 580 W/cm^2. Wong et al. [7] studied the performance of a novel vapor chamber. Parallel grooves are made on the inner surface of the top plate, with inter-groove openings. A layer of

* Corresponding author. Tel./fax: +86 1061772268.
E-mail address: xjl@ncepu.edu.cn (J. Xu).

0017-9310/$ - see front matter © 2012 Elsevier Ltd. All rights reserved.
http://dx.doi.org/10.1016/j.ijheatmasstransfer.2012.04.018

Nomenclature

A	heating area (m^2)
a_0 and a_1	empirically determined constants for temperature distribution in copper block
k	thermal conductivity of solid copper (W/(m K))
L_{fin}	fin height (m)
L_p	cross-section perimeter of the fin (m)
q	heat flux (W/m^2)
Q	heating power recorded from the power meter (W)
R	thermal resistance (K/W)
T	temperature (K or °C)
r	cylindrical coordinate (m)
z	axial coordinate along the fin height direction (m)

Greek symbols

α	forced convection heat transfer coefficient W/m^2 K
ϕ	charge ratio
θ	inclination angle
η	fin efficiency

Subscripts

ave	average
air	air environment
base	fin base
fin	fin
real	real
J	junction location between vapor chamber and heating copper block
max	maximum
sub	substrate
VC	vapor chamber

porous wick was sintered on the bottom plate as the evaporator. The peaks of the groove walls directly contact with the wick so that the grooves simultaneously function as vapor path, condenser and supporting structure. The vapor chamber configuration decreases the liquid flow path towards the bottom wick to sustain high anti-dryout capability. The thermal resistance was measured for the heat load from 80 to 300 W with a heating area of 2.1 by 2.1 cm, or 1.1 by 1.1 cm.

Comments on a conventional vapor chamber are summarized as follows: (1) Various porous wicks are proposed to improve the vapor chamber performance, including copper or aluminum powders [8], graphite foam [9], microchannel groove [10], etc. (2) The inner surface of the top chamber plate acts as the condenser. The condensed liquid returns to the heating area through the side wall of the chamber. The conventional design has a limited condensation area, and the liquid flow path is long, causing the decreased anti-dryout capability for a vapor chamber. (3) A vapor chamber evens the temperature distribution along the radial direction. But the fin heat sink does have a higher temperature on the fin base but a lower temperature at the fin tip, reducing the fin efficiency along the fin height direction. This is the reason why fins should have limited fin height. (4) There is a contact thermal resistance between the vapor chamber and the attached heat sink, which has important contribution to the whole thermal resistance of the cooling system, especially for high heat flux condition.

In this study, a novel vapor chamber using the extended condenser concept, called extended vapor chamber (EVC), was proposed. The vapor chamber and the plate fin pieces ingeniously possess an integrated design. The vapor chamber consists of an evaporator part and an extended condenser part. A layer of compressed copper foam was sintered on the bottom plate as the evaporator. The extended condenser part consists of a circular-straight groove network and a set of fin pieces. The peaks of the groove walls directly contact with the flat copper foam wick (evaporator). Thus the grooves simultaneously act as the vapor path, condenser, and supporting structure. The major modification to the conventional design is to arrange a set of capillary holes within fin pieces. A sliced copper foam bar was inserted in each of the capillary hole. The peaks of the copper foam bar also directly contact with the flat copper foam wick (evaporator). The EVC has the following advantageous: sufficient liquid supply towards the evaporator surface, high fin efficiency and no contact thermal resistance between the vapor chamber and the fin region.

2. The vapor chamber design and its size

The EVC consists of an evaporator part and an extended condenser part (see Fig. 1(a)). There is a copper foam layer with its thickness of 1.0 mm sintered on the bottom plate as the evaporator. The 1.0 mm thickness porous wick was compressed from 2.0 mm thickness copper foam. The condenser part consists of a circular-straight groove network and a set of fins (see Fig. 1a). The groove network has a depth of 3.0 mm, with widths of 2.0 mm for the groove wall and 3.0 mm for the groove channel. Two straight channels are crossed at the central location perpendicularly with each width of 6.0 mm. The width of other two straight channels is 2.0 mm. The 6.0 mm width groove has an angle of 45° with respect to the 2.0 mm width groove. The groove network connects all the vapor channels, distributing the generated vapor everywhere in the chamber (including the capillary holes within fins). The peaks of the groove walls directly contact with the flat copper foam wick (evaporator). The groove network functions as the vapor flow path and supporting structure. It is shown that liquid supply in the heating area is mainly fed by the capillary action of the copper foam bar in capillary holes and flat copper foam wick (evaporator), it is not necessary to use very small groove size here.

The major modification to the conventional design is to arrange a set of capillary holes in the fin region (see Fig. 1(b)). A sliced copper foam bar was inserted in each capillary hole. The peaks of the copper foam bar directly contact with the flat copper foam wick (evaporator). Such a design ensures the whole fin region acted as the condenser. The condensed liquid returns to the flat copper foam wick (evaporator) by the capillary action of the copper foam bar.

The vapor chamber has an overall height of 44.0 mm with a fin height of 37.0 mm (see Fig. 1b). It has a footprint size of 95.0 mm in diameter. There are eleven fin pieces totally. Except the two rim fin pieces, each fin piece has a width of 6.0 mm, with a gap of 3.0 mm between two neighboring fins. There are 95 capillary holes machined in the 9 fin pieces. Each hole has a diameter of 2.0 mm. The copper foam bar inserted in each capillary hole has a rectangular cross-section with its size of 1.0 mm by 1.0 mm.

The copper foam used for the porous wick has a porosity of 0.95 and ppi (pores per inch) of 90. It is a new type of heat transfer material that has been studied extensively in recent years. Some characteristic parameters of the copper foam can be found in Ji et al. [11]. The copper heating block was soldered with the bottom

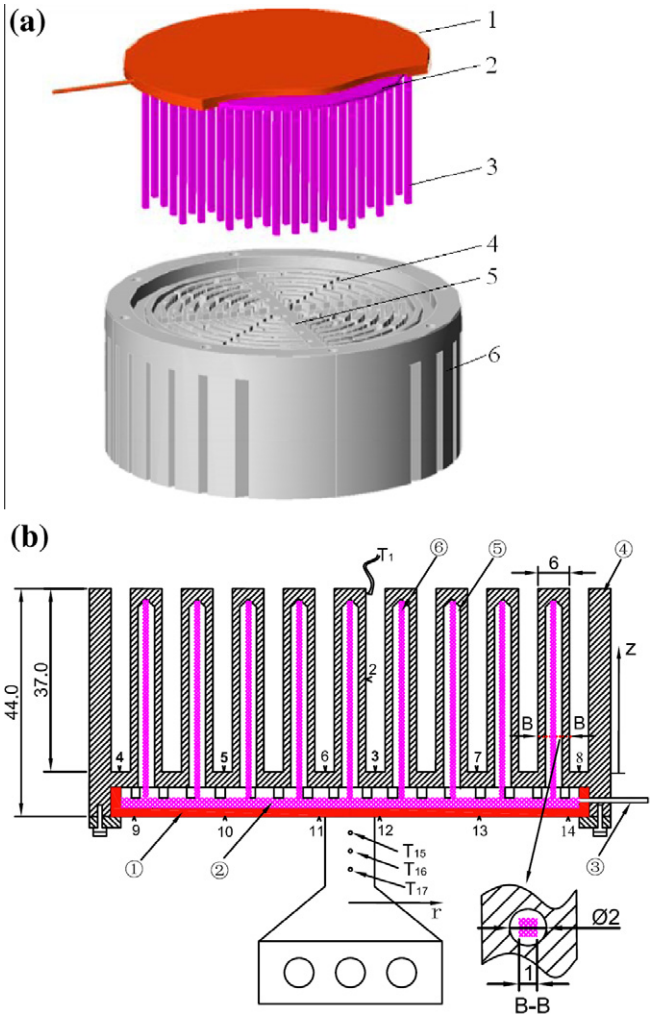

Fig. 1. The EVC design ((a) 1. chamber substrate, 2. compressed copper foam piece, 3. rectangular copper foam bar, 4. groove network, 5. capillary hole, 6. fin) and geometry, size and thermocouple arrangement for the EVC ((b) ①. chamber substrate, ②. flat copper foam wick, ③. fill tube, ④. fin, ⑤. capillary hole, ⑥. rectangular copper foam bar, other numbers are for thermocouple locations).

plate of the vapor chamber (see Fig. 1(b)). Three cartridge heaters driven by a stable AC power supply provide the heating power to the vapor chamber. The heating area is 0.785 cm^2. In Fig. 1(b), T_1–T_3 identify the temperature variation along the fin height. T_4–T_8 are welded on the fin base. T_9–T_{14} are welded on the bottom evaporator surface. Three thermocouple wires inserted in the heating element holes are marked as T_{15}–T_{17}.

3. Experimental procedure and data reduction

Detailed description of the experimental setup can be found in Ji et al. [11]. Heat flux is decided by $q = Q/A$, where Q is the heating power, A is the heating area of 0.785 cm^2. q is also written as $q = -k\frac{dT}{dz}|_J$, where k is the temperature dependent thermal conductivity of copper, $\frac{dT}{dz}|_J$ is the temperature gradient at the junction location. A least square correlation of temperatures versus z was written as $T = a_0 + a_1 z$ based on T_{17}, T_{16} and T_{15} (see Fig. 1(b)). The maximum substrate temperature ($T_{sub,max}$) is determined based on the correlation. The thermal resistance is the temperature difference between the maximum substrate temperature and the average temperature on the fin base, that is $R_{VC} = (T_{sub,max} - T_{ave,base})/Q$, where $T_{ave} = (T_3 + T_4 + T_5 + T_6 + T_7 + T_8)/6$. The fin efficiency characterizes the temperature uniformity along the fin height direction, which is defined as the real dissipated heating power divided by that assuming a uniform temperature along the fin height with the temperature at the fin base:

$$\eta_{fin} = \frac{Q_{real}}{Q_{base}} = \frac{\int_0^{L_{fin}} \alpha(T - T_{air}) L_p dz}{\alpha(T_3 - T_{air}) L_p L_{fin}} \approx \frac{(T_1 + T_2 + T_3)/3 - T_{air}}{T_3 - T_{air}} \quad (1)$$

The standard uncertainty analysis gives uncertainty of the thermal resistances of 6.4%.

4. Results and discussion

Usually the thermal resistance of vapor chambers can be separated into the components for the evaporator and condenser, respectively. Few studies obtained the two components from the total thermal resistance of the vapor chamber [6,7]. However, separation of the thermal resistance of vapor chambers needs to measure the fluid temperature inside the vapor chamber. It is difficult to ensure the high sealing to prevent the air leakage from the environment to the vapor chamber. Thus most of vapor chamber studies use the thermal resistance of the vapor chamber to characterize its performance [9,12]. The thermal resistance of vapor chambers usually does not include the contribution from the fin heat sink. The objective of this study is to compare the thermal resistance of the EVC with other studies, not including the thermal resistance of the fin region. The studies are to identify the thermal resistance of the chamber section and the maximum heat flux that can be sustained by the EVC.

We compare the extended vapor chamber data with other studies in Fig. 2(a). Wong et al. [7] studied a novel vapor chamber, showing smaller liquid flow resistance and hence high anti-dryout capability. Fig. 2(a) plots the thermal resistances versus heat fluxes for the heating area of 1.21 and 4.41 cm^2 with water as the working fluid. The minimum thermal resistance of 0.16 K/W is reached at the heat flux of 124 W/cm^2, beyond which the thermal resistances are sharply increased to indicate the dryout phenomenon. Horiuchi et al. [13] studied the vapor chamber using microchannel wick instead of sintered powder wick. A minimum thermal resistance of 0.17 K/W is reached at the heat flux of 135 W/cm^2, beyond which the thermal performance becomes worse.

Chen et al. [14] developed a vapor chamber using diamond-copper composition as the wick structure. Three diamond-to-copper powder volume ratios of 1/4, 1/6 and 1/8 were used to fabricate the wick sheets and columns. The authors stated that the diamond-copper powder wick effectively prevents the dryout at high heat fluxes. The tested heat fluxes are smaller than 57 W/cm^2 (see Fig. 2(a)). The minimum thermal resistance occurs at $q = 38$ W/cm^2 for the diamond to copper powder volume ratio of 1/6.

Zhao and Chen [15] introduced a high performance vapor chamber heat spreader with a novel bi-dispersed wick structure. The main wick structure is a sintered porous network in a latticed pattern, containing not only small pores to transport liquid by capillary forces, but also many slots to provide large passages to vent vapor from heated surfaces. The copper particles had a diameter of approximately 50 μm, and an effective pore radius of approximately 13 μm after sintering was obtained. The slots had a typical width of approximately 500 μm. It was shown by the experiments that vapor chamber heat spreaders with the latticed wicks present three times improvement on heat spreading performance, comparing with a solid copper heat spreader, and much improved capacity to handle hot spots with local heat fluxes exceeding 300 W/cm^2 at a heating area of 0.25 cm^2.

Seeing from Fig. 2(a), the extended vapor chamber here not only enlarges the operating range of heat fluxes, but also delays the transition point for dryout, significantly. The tested heat flux is

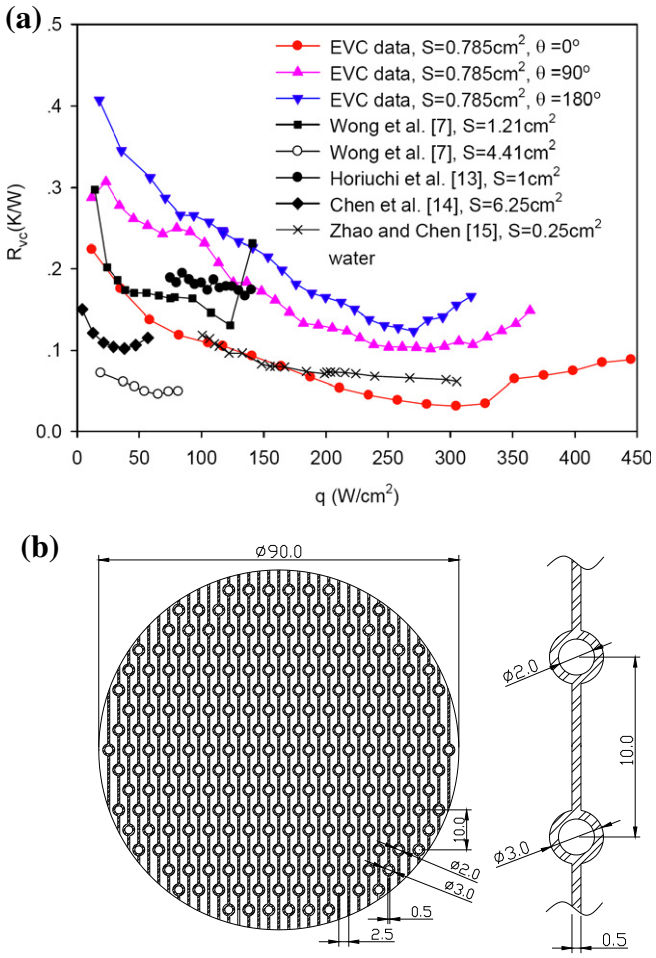

Fig. 2. The thermal resistances of the present EVC and comparison with other studies (a) and a tube panels design in the fin region (b).

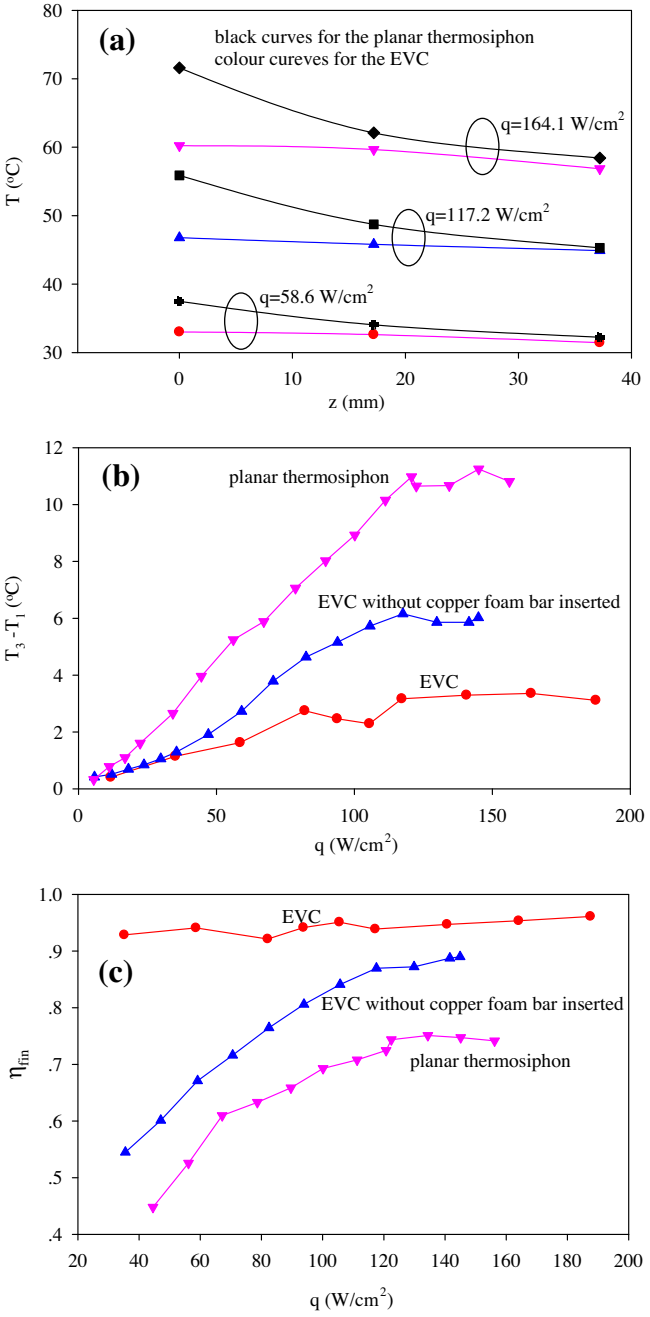

Fig. 3. Temperatures along the fin height direction and fin efficiency ($\theta = 0°$, $\phi = 0.3$.

up to 445 W/cm^2 but without indicating apparent dryout. The extended vapor chamber has the smallest thermal resistances than those reported in the literature for the bottom heating ($\theta = 0°$). Chen et al. [14] obtained smaller thermal resistance than EVC for bottom heating but their studies covered a narrow heat flux range of smaller than 57 W/cm^2.

Even though the Zhao and Chen [15] studies covered a heat flux range of 300 W/cm^2, but the heater area used was 0.25 cm^2, which is one-third of the present heater area. The present EVC can be used not only for ultra-high heat fluxes, but also for larger heater area. Fig. 2(a) gave the EVC data for side heating ($\theta = 90°$) and top heating ($\theta = 180°$). It is noted that most of the experimental data are reported for the bottom heating ($\theta = 0°$) in the literature. Few studies such as Wong et al. [7] studied the effect of inclination angles on the thermal performance of vapor chambers.

The improved thermal performance of this EVC is due to the following mechanisms. The cooper foam has a high porosity of 0.95, which is larger than the porosity of 0.3–0.6 for conventional porous media. The high porosity ensures a larger foam thickness used and decreases the flow resistance of the two-phase circulation in the vapor chamber. Due to the distinct nature of the metallic foam, multiscale pore sizes existed. The larger pores help to release the created vapor while the smaller pores help to suck the liquid towards the heater surface, decreasing the shear stress at the vapor–liquid interface for the counter-current flow. The major modification of this study is to insert copper foam bars in the capillary holes within the plate fins. The fin region not only acts as the heat sink to dissipate the heat to the environment, but also acts as the condensation sections of heat pipes. The phase change heat transfer in capillary holes within fin pieces ensures uniform temperatures along the fin height direction to significantly increase the fin efficiency. At the same fin area exposed in the air environment, more heat can be dissipated. Because the copper foam bars directly contact with the evaporator porous surface, sufficient liquid flow rate can be supplied towards the evaporator (heating) surface, significantly delaying the appearance of dryout. This is the major reason why the present EVC can sustain high heat flux.

This is a preliminary study of the extended vapor chamber. The present EVC had smaller fin area than conventional fin heat sinks. This disadvantage can be overcome by using the tube panels configuration in the fin region (see Fig. 2(b)). There are 35 fin pieces arranged in a footprint area with its diameter of 90.0 mm. Each fin piece has a thickness of 0.5 mm and a gap distance of 2.0 mm with

its neighboring fin piece. A set of capillary tubes were integrated with each fin piece. The outer and inner diameters of the capillary tube are 3.0 and 2.0 mm, respectively. If the capillary tube is filled with copper foam bar with the rectangular cross section, the capillary tube acts as a miniature heat pipe, which not only evens the temperature distribution along the fin height direction to increase the fin efficiency, but also pumps the liquid towards the evaporator heating surface. The fin material is aluminum. The proposed tube panels design can be fulfilled by the widely used casting technique, thus the fabrication cost is acceptable. The EVC using the tube panels design will be tested by future experiment.

In order to compare the temperatures on the fin surface with and without capillary holes within fin piece, we fabricated a planar thermosiphon integrated with the fin region, which had exactly identical configuration and dimensions with the EVC, except that there are no capillary holes within fin pieces. Even though there are no porous wicks on the top surface of the planar thermosiphon, there are miniature rectangular channels on the top chamber surface (see Fig. 1(a)), which act as the condenser surface and induce liquid towards the evaporator heating surface. Actually the planar thermosiphon is a type of vapor chamber, similar to the design of Wong et al. [7,16].

Fig. 3(a) indicates that the EVC significantly evens the temperature distribution on the fin surface compared with the planar thermosiphon. Both EVC and planar thermosiphon had almost identical temperatures at the fin tip (z = 37.0 mm). But EVC had much lower temperatures than the planar thermosiphon at the fin base. At q = 164.1 W/cm^2, the temperature for EVC is lower by 11 °C than that for the planar thermosiphon on the fin base (see Fig. 3(a)). $T_3 - T_1$ is the temperature difference between the fin base and tip, which has a linear increase versus heat fluxes and attains 11 °C at q = 120–150 W/cm^2 for the planar thermosiphon (see Fig. 3(b)). Quite small temperature difference of $T_3 - T_1$ is identified for EVC, which is less than 3.4 °C at q = 100–190 W/cm^2. EVC without inserted copper foam bar has larger $T_3 - T_1$ than EVC, but smaller $T_3 - T_1$ than the planar thermosiphon. Fig. 3(c) gave a nearly constant fin efficiency of 0.93 at q = 0–200 W/cm^2 for EVC. But the planar thermosiphon has quite smaller fin efficiencies than the EVC. The EVC without inserted copper foam bar has increased fin efficiencies versus heat fluxes and attains 0.89 at q = 140 W/cm^2. The above finding shows that the condensation heat transfer within capillary holes evens the temperature distribution along the fin height direction. The inserted copper foam bar further improves the fin performance. The extended condenser concept has the potential to reduce the surface area and size of fin heat sinks.

Charge ratio is defined as the liquid volume divided by the total inside volume for an EVC, which is an important parameter to influence the thermal performance. If the charge ratio is too small, the evaporator surface can be easily dryout. If the charge ratio is too large, the liquid will block the vapor channel. Thus an ideal charge ratio shall ensure the complete wet of the porous wick on the evaporator surface and does not increase the flow resistance of the vapor flowing towards the condenser surface. Based on our previous studies [11], the suitable charge ratio has a range of 0.1–0.4. Fig. 4 shows the combined effects of the charge ratios and inclination angles on the thermal resistances of the EVC. At four inclination angles of 0°, 60°, 90° and 180°, the charge ratio of 0.3 is almost the optimal value for EVC applications. Inclination angles and charge ratios are combined to affect the thermal performance of vapor chambers. For the bottom heating, there are no much differences of thermal resistances among various charge ratios, except the lowest thermal resistance reached by the charge ratio of 0.3 (see Fig. 4(a)). With inclined positions of EVC such as θ = 60° and 90°, the sensitivity of thermal resistances on charge ratios is decreased, i.e., the thermal resistance differences among various charge ratios are decreased (see Fig. 4(b) and (c)). For top heating (θ = 180°), the phenomenon is complicated. Charge ratios of 0.2 and 0.4 gave higher thermal resistances, and charge ratios of 0.15 and 0.3 gave lower thermal resistances (see Fig. 4(d)). Curves of thermal resistances versus heat fluxes are crossed with each other at heat fluxes exceeding 100 W/cm^2.

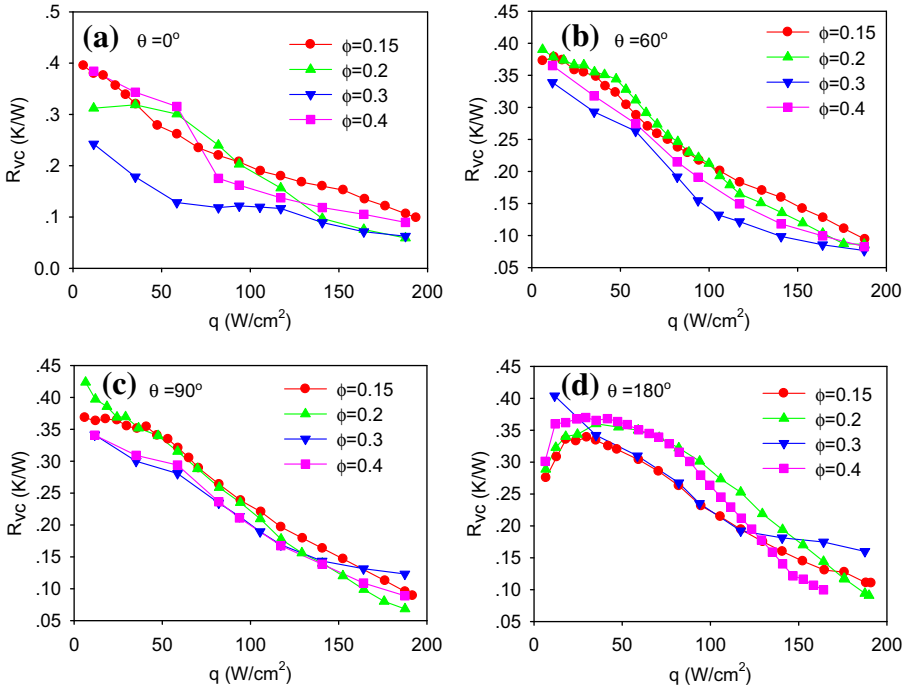

Fig. 4. Effect of fill ratios and inclination angles on the thermal resistance.

5. Conclusions

A vapor chamber based on extended condenser concept was proposed. The EVC consists of an evaporator part and an extended condenser part, having an integrated design of the chamber and fin region. A layer of compressed copper foam was sintered on the inner evaporator surface. The condenser part consists of a circular-straight groove network and fin region. The groove network connects all the vapor channels, distributing generated vapor everywhere in the internal volume of the vapor chamber. The major modification to the conventional design is to machine a set of capillary holes within solid fins. A sliced copper foam bar with a rectangular cross section is inserted in each of capillary hole. The peaks of copper foam bar are tightly contacted with the flat copper foam piece (evaporator). It is found that a minimum thermal resistance of 0.03 K/W was reached for bottom heating. The maximum tested heat flux was up to 445 W/cm^2 without reaching any dryout. EVC significantly delays the transition point of thermal resistances versus heat fluxes with the heat flux exceeding 300 W/cm^2. Thermal resistances are only slightly increased beyond such transition point. Considering heat flux and heater area, the EVC thermal performance is the best by comparing with other studies in the literature. EVC can be used for ultra-high heat flux and larger heater area conditions. EVC evens the temperature distribution along the fin height direction. The high fin efficiency of 0.93 indicates the great potential to reduce the fin surface area and size. Inclination angles and charge ratios are combined to affect the thermal performance of EVC. An optimal charge ratio of 0.3 was recommended.

Acknowledgements

This work was supported by the Joint Fund of the National Natural Science Foundation of China and Guangdong Province (U1034004), Natural Science Foundation of China for distinguished young scholars (50825603), the National Basic Research Program of China (2011CB710703), and the Beijing Science and Technology Program (Z111109055311097).

References

[1] M.P. Arik, J. Weaver, Thermal challenges in the future generation solid state lighting applications: light emitting diodes, in: Proceedings of IEEE Intersociety Conference on Thermal Phenomena, San Diego, USA, 2002.
[2] H. Agata, F. Kiyooka, M. Mochizuki, K. Mashiko, Y. Saito, Y. Kawahara, T. Nguyen, T. Nguyen, Advance Thermal solution using vapor chamber technology for cooling high performance desktop CPU in notebook computer, in: The 1st International Symposium on Micro and Nano Technology, Honolulu, Hawaii, USA, March 4–17, 2004.
[3] X.P. Wu, M. Mochizuki, N. Thang, Y. Saito, V. Wuttijumnong, H. Ghisoiu, V. Kumthonkittikul, P. Sukkasaem, P. Nimitkiatklai, F. Kiyooka, A.I. Fujikura, N.C. Raleigh, Low profile-high performance vapor chamber heat sinks for cooling high-density blade servers, in: 23rd IEEE SEMI-THERM Symposium, San Jose, CA, March 20–22, 2007.
[4] K. Take, Y. Furukawa, S. Ushioda, Fundamental investigation of roll bond heat pipe as heat spreader plate for notebook computers, IEEE Trans. Compon. Pack. Technol. 23 (2000) 80–85.
[5] S.H.K. Lee, S.K. Chu, C.C.C. Choi, Y. Jaluria, Performance characteristics of vapor chambers with boiling enhanced multi-wick structures, in: 23rd IEEE SEMI-THERM Symposium, San Jose, CA, March 20–22, 2007.
[6] G.S. Hwang, E. Fleming, B. Carne, S. Sharratt, Y. Nam, P. Dussinger, Y.S. Ju, M. Kaviany, Multi-artery heat-pipe spreader: lateral liquid supply, Int. J. Heat Mass Transfer 54 (2011) 2334–2340.
[7] S.C. Wong, K.C. Hsieh, J.D. Wu, W.L. Han, A novel vapor chamber and its performance, Int. J. Heat Mass Transfer 53 (2010) 2377–2384.
[8] Y.M. Xuan, Y.P. Hong, Q. Li, Investigation on transient behaviors of flat plate heat pipes, Exp. Therm. Fluid Sci. 28 (2004) 249–255.
[9] M.H. Lu, L. Mok, R.J. Bezama, A graphite foams based vapor chamber for chip heat spreading, J. Electron. Packag. 128 (2006) 427–431.
[10] R. Hophins, A. Faghri, D. Khrustalev, Flat miniature heat pipe with micro capillary grooves, J. Heat Transfer, Trans. ASME 121 (1999) 102–109.
[11] X.B. Ji, J.L. Xu, A.M. Abanda, Copper foam based vapor chamber for high heat flux dissipation, Exp. Therm. Fluid Sci. (2012), http://dx.doi.org/10.1016/j.expthermflusci.2012.02.004.
[12] H.Y. Li, M.H. Chiang, C.I. Lee, W.J. Yang, Thermal performance of plate-fin vapor chamber heat sinks, Int. Commun. Heat Mass Transfer 37 (2010) 731–738.
[13] Y. Horiuchi, M. Mochizuki, K. Mashiko, Y. Saito, Micro channel vapor chamber for high heat Spreading, in: 10th Electronics Packaging Technology Conference, 2008, pp. 749–754.
[14] Y.T. Chen, J.M. Miao, D.Y. Ning, T.F. Chu, W.E. Chen, Thermal performance of a vapor chamber heat pipe with diamond-copper composition wick structures, in: International Microsystems, Packaging, Assembly and Circuits Technology Conference, 2009, pp. 340–343.
[15] Y. Zhao, C.L. Chen, Development of a high performance vapor chamber for high heat flux applications, in: Proceedings of MNHT Micro/Nanoscale Heat Transfer International Conference, Tainan, Taiwan, January 6–9, 2008.
[16] S.C. Wong, S.F. Huang, K.C. Hsieh, Performance tests on a novel vapor chamber, Appl. Therm. Eng. 31 (2011) 1757–1762.